

Loss of function mutations in *HARS* cause a spectrum of inherited peripheral neuropathies

Dana Safka Brozkova,¹ Tine Deconinck,^{2,3} Laurie Beth Griffin,^{4,5} Andreas Ferbert,⁶ Jana Haberlova,¹ Radim Mazanec,⁷ Petra Lassuthova,¹ Christian Roth,⁶ Thanita Pilunthanakul,⁸ Bernd Rautenstrauss,^{9,10,†} Andreas R. Janecke,¹¹ Petra Zavadakova,¹² Roman Chrast,¹² Carlo Rivolta,¹² Stephan Zuchner,¹³ Anthony Antonellis,^{4,14,15} Asim A. Beg,⁸ Peter De Jonghe,^{2,3,16} Jan Senderek,^{10,*} Pavel Seeman^{1,*} and Jonathan Baets^{2,3,16,*}

[†]Deceased.

*These authors contributed equally to this work.

Inherited peripheral neuropathies are a genetically heterogeneous group of disorders characterized by distal muscle weakness and sensory loss. Mutations in genes encoding aminoacyl-tRNA synthetases have been implicated in peripheral neuropathies, suggesting that these tRNA charging enzymes are uniquely important for the peripheral nerve. Recently, a mutation in histidyl-tRNA synthetase (*HARS*) was identified in a single patient with a late-onset, sensory-predominant peripheral neuropathy; however, the genetic evidence was lacking, making the significance of the finding unclear. Here, we present clinical, genetic, and functional data that implicate *HARS* mutations in inherited peripheral neuropathies. The associated phenotypic spectrum is broad and encompasses axonal and demyelinating motor and sensory neuropathies, including four young patients presenting with pure motor axonal neuropathy. Genome-wide linkage studies in combination with whole-exome and conventional sequencing revealed four distinct and previously unreported heterozygous *HARS* mutations segregating with autosomal dominant peripheral neuropathy in four unrelated families (p.Thr132Ile, p.Pro134His, p.Asp175Glu and p.Asp364Tyr). All mutations cause a loss of function in yeast complementation assays, and p.Asp364Tyr is dominantly neurotoxic in a *Caenorhabditis elegans* model. This study demonstrates the role of *HARS* mutations in peripheral neuropathy and expands the genetic and clinical spectrum of aminoacyl-tRNA synthetase-related human disease.

- 1 DNA Laboratory, Department of Paediatric Neurology, 2nd Faculty of Medicine, Charles University in Prague and Motol University Hospital, Prague 150 06, Czech Republic
- 2 Neurogenetics Group, VIB-Department of Molecular Genetics, University of Antwerp, Antwerpen 2610, Belgium
- 3 Laboratory of Neurogenetics, Institute Born-Bunge, University of Antwerp, Antwerpen 2610, Belgium
- 4 Cellular and Molecular Biology Program, University of Michigan Medical School, Ann Arbor, MI-48109, USA
- 5 Medical Scientist Training Program, University of Michigan Medical School, Ann Arbor, MI-48109, USA
- 6 Department of Neurology, Klinikum Kassel, Kassel 34125, Germany
- 7 Department of Neurology, 2nd Faculty of Medicine, Charles University in Prague and Motol University Hospital, Prague 150 06, Czech Republic
- 8 Department of Pharmacology, University of Michigan Medical School, Ann Arbor, MI-48109, USA
- 9 Medizinisch Genetisches Zentrum, Munich 80335, Germany
- 10 Friedrich-Baur-Institute, Department of Neurology, Ludwig-Maximilians-University, Munich 80336, Germany
- 11 Division of Human Genetics and Department of Pediatrics I, Medical University of Innsbruck, Innsbruck 6020, Austria
- 12 Department of Medical Genetics, University of Lausanne, Lausanne 1005, Switzerland

Received February 19, 2015. Revised March 29, 2015. Accepted April 17, 2015. Advance Access publication June 13, 2015

© The Author (2015). Published by Oxford University Press on behalf of the Guarantors of Brain. All rights reserved.

For Permissions, please email: journals.permissions@oup.com

- 13 Dr John T McDonald Foundation Department of Human Genetics, John P Hussman Institute for Human Genomics, University of Miami Miller School of Medicine, Miami, FL-33136, USA
 14 Department of Human Genetics, University of Michigan Medical School, Ann Arbor, MI-48109, USA
 15 Department of Neurology, University of Michigan Medical School, Ann Arbor, MI-48109, USA
 16 Department of Neurology, Antwerp University Hospital, Antwerpen 2610, Belgium

Correspondence to: Pavel Seeman,
 DNA laboratory,
 Department of Paediatric Neurology,
 V Úvalu 84, 150 06,
 Praha 5,
 Czech Republic
 E-mail: pseeman@yahoo.com

Keywords: hereditary motor and sensory neuropathies; molecular genetics; neurodegeneration; RNA processing; whole-exome sequencing

Abbreviations: ARS = aminoacyl-tRNA synthetase; CMT = Charcot–Marie–Tooth; HMN = hereditary motor neuropathy; HMSN = hereditary motor and sensory neuropathy; IPN = inherited peripheral neuropathy

Introduction

Inherited peripheral neuropathies (IPNs) represent a common, heterogeneous group of disorders that affect about 1 in 2500 individuals worldwide (Skre, 1974). A common feature of these diseases is progressive, length-dependent axonal degeneration of the peripheral nervous system resulting in impaired motor and sensory function in the distal extremities. IPNs are clinically subdivided based on the involvement of different types of peripheral nerve fibres. The most common type is hereditary motor and sensory neuropathy (HMSN), also known as Charcot–Marie–Tooth (CMT) disease, which affects both motor and sensory fibres. Less frequent subtypes display more selective involvement of nerve fibres and include hereditary motor neuropathy (HMN) and hereditary sensory and autonomic neuropathy (HSAN). The common HMSN/CMT group is further classified based on electrophysiological studies with motor nerve conduction velocities in the median nerve <38 m/s (normal >49 m/s) indicating demyelinating neuropathy (CMT1 or HMSN-I) and nerve conduction velocities >38 m/s indicating axonal neuropathy (CMT2 or HMSN-II) (Harding and Thomas, 1980). In addition, an intermediate group is defined as having nerve conduction velocities between 25 and 45 m/s among patients in the same family (Baets *et al.*, 2014). Interestingly, IPNs display a high level of clinical heterogeneity, even among patients that carry an identical genetic lesion.

The genetic diversity of IPN is extensive with >75 genes identified to date (Baets *et al.*, 2014). The transmission of the disease can be autosomal dominant, autosomal recessive, or X-linked. Dominantly inherited CMT1 is the most common type and also the easiest to diagnose genetically with mutations in three loci accounting for at least 80% of cases (Saporta *et al.*, 2011; Rossor *et al.*, 2013). In contrast, for axonal forms (CMT2) the genetic cause is only found in ~25% of patients because there are no major gene(s) accounting for a substantial proportion of patients

(with the possible exception of mitofusin 2, *MFN2*), and the locus and allelic heterogeneity of CMT2 is extensive with many genes still undiscovered (Murphy *et al.*, 2012).

Aminoacyl-tRNA synthetases (ARSs) are ubiquitously expressed, essential enzymes that charge tRNA molecules with cognate amino acids—the first step of protein translation (Antonellis and Green, 2008). To date, mutations in six genes encoding ARSs have been identified in patients with IPN phenotypes (Antonellis *et al.*, 2003; Jordanova *et al.*, 2006; Latour *et al.*, 2010; McLaughlin *et al.*, 2010; Gonzalez *et al.*, 2013a; Vester *et al.*, 2013). Three of these genes have been convincingly implicated in disease via linkage analysis, with multiple families and patients described in independent studies: (i) glycyl-tRNA synthetase mutations (*GARS*) cause CMT2D and HMN5A (Antonellis *et al.*, 2003); (ii) tyrosyl-tRNA synthetase mutations (*YARS*) cause an intermediate form of CMT (DI-CMTC) (Jordanova *et al.*, 2006); and (iii) alanyl-tRNA synthetase mutations (*AARS*) cause CMT2N and also a form of HMN (Latour *et al.*, 2010; Zhao *et al.*, 2012). Interestingly, extensive functional studies have shown that disease-associated ARS mutations cause a loss-of-function effect in tRNA charging and yeast viability assays, suggesting that peripheral nerves are uniquely sensitive to tRNA charging deficits (Wallen and Antonellis, 2013).

Recently, a p.Arg137Gln variant in the histidyl-tRNA synthetase gene (*HARS*) was found by whole exome sequencing in an isolated patient with a sporadic, late-onset predominantly sensory axonal neuropathy (Vester *et al.*, 2013). While functional studies in yeast revealed that the variant behaved similarly to other disease-implicated ARS variants, the lack of convincing genetic findings and the detection of the variant in the general population made it impossible to conclude that this was a disease-causing mutation (Vester *et al.*, 2013). Here, we present 23 patients from four unrelated families with *HARS* mutations that segregate with axonal or intermediate neuropathy phenotypes. Our functional studies show that all identified

mutations are unable to support viability in yeast complementation assays and that one mutation is dominantly toxic in a worm model system. Combined, our data clearly establish *HARS* as a neuropathy-associated locus and further expand the genetic and phenotypic spectrum of ARS-related human disease.

Patients and methods

Patients

In total, 23 patients from four unrelated families with a dominantly inherited peripheral neuropathy are described (Fig. 1). The Ethical Review Boards of the participating institutions approved this study. All patients or their legal representatives signed informed consent prior to enrolment.

Linkage analysis

To define the molecular genetic basis of the disease in Families A and D, a whole genome scan using single nucleotide polymorphism (SNP) arrays was carried out. Genomic DNA samples from patients and unaffected relatives were hybridized to GeneChip® Human Mapping NspI 250 K arrays (Family A, seven individuals) and GeneChip® Human Mapping 50 K arrays (Family D, 12 individuals) (Affymetrix) according to the manufacturer protocols. Genotypes were called using GeneChip® Genotyping Analysis Software (Version 4.1) and default thresholds. To identify the linkage regions, the parametric multipoint logarithm of the odds (LOD) scores and haplotypes were obtained using a subset of SNPs (distance between markers >50 kb and heterozygosity >0.15) with

the MERLIN program (v 1.1.2) with the assumption of an autosomal dominant mode of inheritance and fully penetrant model (Abecasis *et al.*, 2002).

For Family B, an in-house developed multiplex genome-scan panel was used consisting of 422 polymorphic short tandem repeat (STR) markers, subsequently PCR amplified with fluorescently labelled primers and size-separated on an ABI3730xl DNA Analyzer. Results were scored with an in-house developed software program, Local Genotype Viewer (LGV). Two-point parametric linkage analysis was calculated with EasyLINKAGE software package under a fully penetrant autosomal dominant model, equal female/male recombination rates, and a disease frequency of 0.0001.

Sanger sequencing

Prior to linkage analysis, candidate gene sequencing, or whole-exome sequencing, the chromosome 17 duplication (CMT1A) was excluded in all four families. Subsequently, various sets of IPN associated genes were tested negative in these families: *GJB1*, *MPZ*, *BSCL2*, *NEFL*, *MFN2*, *HSP22*, *HSP27*, *RAB7*, *GARS*, *YARS*, *DNM2*, and *TRPV4* in Family A; *MPZ*, *PMP22*, *GJB1*, *GARS*, *AARS*, and *GDAP1* in Family B; *PMP22* in Family C; *GJB1*, *MPZ*, *HSP22*, *HSP27*, *SETX*, and *BSCL2* in Family D.

For the index patient of Family A, all 13 coding exons and adjacent exon-intron boundaries of *HARS* were amplified as well as a cohort of 61 index patients with genetically unresolved HMN (primers available upon request). To validate whole-exome sequencing results (Families B, C and D) and to demonstrate segregation, the mutated exons of *HARS* were Sanger sequenced in all available individuals. Primer pairs were designed with the Primer3 program (sequences available upon request) (Rozen and Skaletsky, 2000). Total

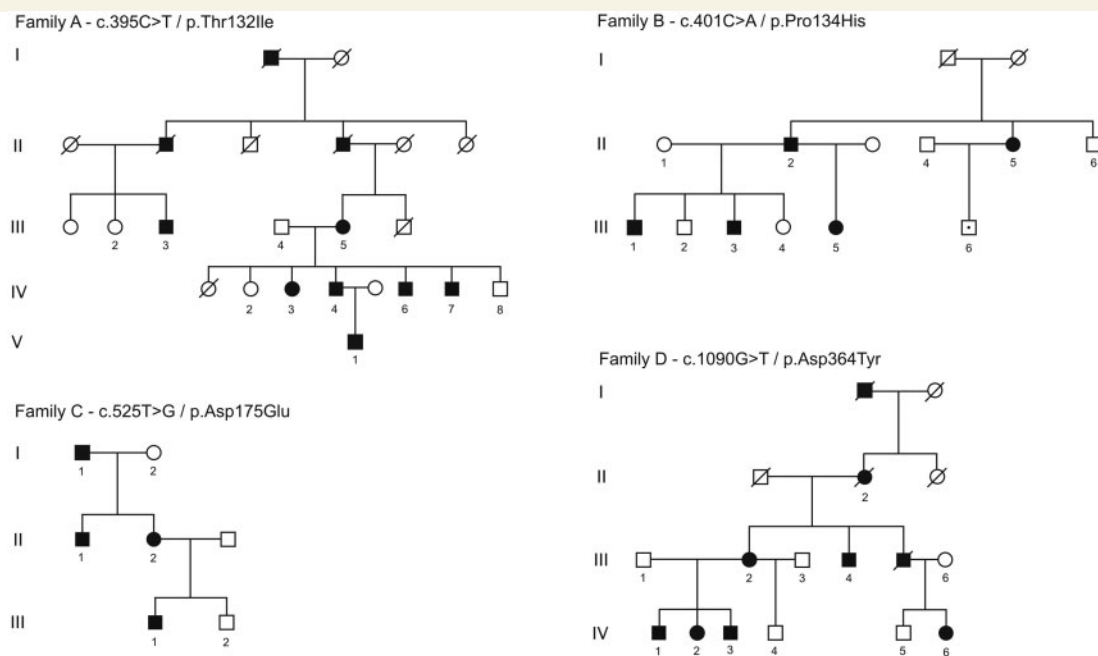


Figure 1 Pedigrees of the families with *HARS* mutations. Female family members are indicated with a circle and male family members are indicated by squares. Filled symbols indicate affected individuals, while empty symbols indicate unaffected individuals. The number of the individual is shown in Arabic numerals if the DNA was available for genotyping.

genomic DNA was PCR amplified and PCR products were bi-directionally sequenced using the BigDye[®] Terminator v3.1 cycle sequencing kit (Applied Biosystems). Fragments were separated on an ABI3730xl and ABI 3130 Genetic Analyzer (Applied Biosystems) and analysed with SeqMan[™] II Software (DNASTar Inc.) and Mutation Surveyor[®] (Softgenetics).

Whole-exome sequencing

Index patients from Families B and C and two distant relatives from Family D (Subjects IV.1 and IV.6) were selected for whole-exome sequencing. Exome capture was performed using the Agilent SureSelect Human All Exon V5 kit (50 Mb), followed by sequencing on a HiSeq 2000 platform (Illumina). Sequence alignment was performed using the BWA-v0.5.9rc1 tool. GATK-v1.4-37 was used for variant calling. Further data analysis was performed in the Genomes Management Application database (GEM-app) (Gonzalez *et al.*, 2013b). Variants were filtered for the regions with suggestive linkage for Families B and D, no occurrence in the normal population [absent in the Exome Variant Server (EVS)], predicted impact on the encoded protein (missense, nonsense, frame shift, inframe indels and essential splice variants), conservation [Genomic Evolutionary Rate Profiling (GERP) score > 4, or PhastCons score > 0.9, or PhyloP Score > 1.5], and predicted damaging amino acid substitution [at least in one: SIFT, PolyPhen-2, MutationTaster, Mutation Assessor, Likelihood Ratio Test (LRT), Functional Analysis through Hidden Markov Models (FATHMM)], and quality (GATK GQ score > 75). An overview of the general outcome after performing whole-exome sequencing (number of reads, coverage etc.) can be found in Supplementary Table 1. Confirmation of the possible pathogenic variants and segregation analysis in all available family members was performed using Sanger sequencing.

Yeast complementation assays

Yeast complementation assays were performed as previously described (Vester *et al.*, 2013). Briefly, mutation-containing oligonucleotides were designed to model the p.Thr132Ile, p.Thr132Ser, p.Pro134His, p.Asp175Glu, or p.Asp364Tyr HARS missense variants in the yeast orthologue *HTS1*. The QuickChange[®] II XL Site-Directed Mutagenesis Kit (Stratagene) was used (per manufacturer's instructions) to mutate the *HTS1* locus in a pDONR221 Gateway[®] entry clone (Invitrogen). Resulting clones were purified and sequenced to confirm successful mutagenesis and exclude polymerase-induced mutations. The mutated *HTS1*/pDONR221 entry clone was subsequently recombined into a Gateway[®]-compatible *LEU2*-bearing pRS315 destination vector. Resulting clones were purified and digested with BsrGI (New England Biolabs) to confirm successful recombination.

Two independently generated haploid $\Delta hts1$ strains (harbouring a pRS316 maintenance vector to express wild-type *HTS1* and *URA3*) were transformed with a *LEU2*-bearing pRS315 vector containing no insert ('Empty pRS315' in Fig. 2) or containing a wild-type or mutant *HTS1* allele (Vester *et al.*, 2013). Subsequently, yeast strains were selected

on medium lacking uracil and leucine (Teknova) to select for the presence of both vectors. For each transformation, four colonies were grown to saturation in selective medium for 48 h. Next, 10 μ l of undiluted and diluted (1:10 and 1:100) samples from each culture were spotted on plates containing 0.1% 5-fluoroorotic acid (5-FOA) or SD -leu -ura growth medium (Teknova) and incubated at 30°C for 48 h. Survival was determined by visual inspection of growth. Experiments were performed using two independently generated *HTS1* expression constructs for each allele (designated as 'A' and 'B' in Fig. 2).

Caenorhabditis elegans plasmids and strains

Nematode strains were provided by the *Caenorhabditis* Genetic Centre. Strains were raised at room temperature on nematode growth media plates with OP50 *Escherichia coli* as the food source per standard protocols (Brenner, 1974). Plasmids and transgenic worms were constructed as previously described (Mello *et al.*, 1991; Vester *et al.*, 2013). The human p.Asp364Tyr mutation was created by PCR-based site directed mutagenesis into the equivalent *C. elegans hars-1* residue D383Y using the oligonucleotide primers: D383Y_FWD: TAGCTGCCGGTGGACGATACTAT; and D383Y_REV: ATAGTATCGTCCACCGGCAGCTA.

Morphological and behavioural analysis in C. elegans

Quantification of motor neuron and behavioural defects were performed as previously described (Vester *et al.*, 2013). Quantification was performed on the following strains: EG1285: *oxIs12* (Punc-47::GFP; lin15b) X, BEG16: *oxIs12* (Punc-47::GFP; lin15b) X; aabEx12 (Punc-25::hars-1 [D383Y], Pmyo-2::mCherry). L4 stage worms were synchronized by bleaching and grown at 20°C. Morphological defects were quantitated in >100 worms/genotype at each developmental time point. Animals exhibiting at least one aberrant neuronal process were scored as positive. Behavioural thrash assays were performed as previously described (Miller *et al.*, 1996; Vester *et al.*, 2013). At least 40 animals/genotype were tested. Briefly, single animals were picked to a 35 mm agarose-coated dish filled with 2 ml of M9 media. Animals were allowed to acclimate for 2 min and then a 1-min video was recorded using a Leica IC80HD camera. The movies were slowed to one-quarter speed and the total number of body bends per minute was manually scored offline using ImageJ software.

Microscopy

All morphological quantitation was performed on a Leica DMI6000B compound microscope with a CCD camera (DFX360, Leica Microsystems Inc.) using a $\times 40$ objective. High-resolution confocal images were obtained on a Nikon A1R microscope with a $\times 20$ and $\times 60$ objective (Nikon Corporation).

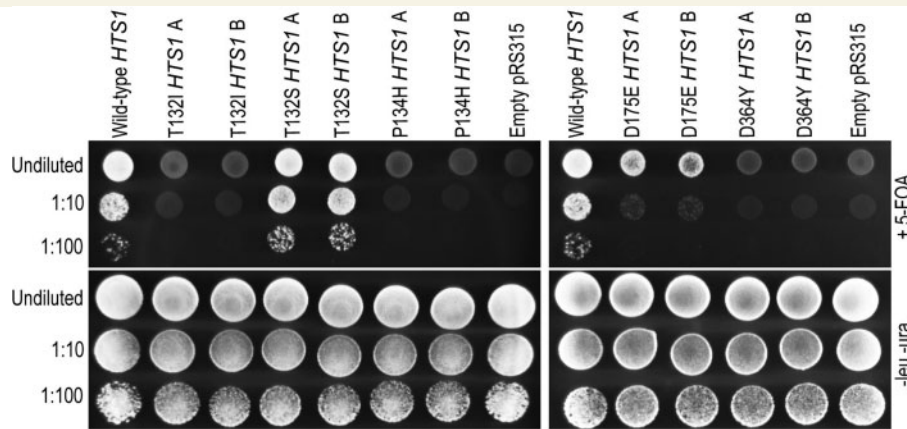


Figure 2 CMT-associated *HTS1* variants decrease yeast cell viability. Haploid $\Delta hts1$ yeast strains were transformed with a vector containing no insert (pRS315 Empty) or an insert to express wild-type, p.Thr132Ile, p.Thr132Ser, p.Pro134His, p.Asp175Glu or p.Asp364Tyr *HTS1* (Supplementary Table 4). Two colonies (indicated by 'A' and 'B') from transformations with Thr132Ile, Thr132Ser, Pro134His, Asp175Glu or Asp364Tyr *HTS1* are shown. Resulting colonies (undiluted, diluted 1:10, or diluted 1:100) were grown on agar plates containing 0.1% 5-FOA. Note the severe depletion of growth associated with p.Asp175Glu *HTS1* at 1:10 and 1:100 dilutions.

Results

Mutations in *HARS* are identified in patients with IPN

Linkage analysis, Sanger sequencing, and whole-exome sequencing revealed four distinct heterozygous mutations in *HARS* in four unrelated families with dominantly inherited peripheral neuropathy.

Genome-wide linkage analysis in Family A, including four affected and three unaffected family members, revealed one chromosomal interval on chromosome 5q tentatively linked to the disease, with a maximal LOD score of 2.107. All affected individuals, but none of the unaffected subjects, shared a haplotype consisting of 93 SNP alleles over a region of 7.9 Mb. This interval contained 161 positional RefSeq genes including *HARS*, which was considered as the most plausible candidate gene (Vester *et al.*, 2013). Sanger-sequencing of *HARS* revealed the p.Thr132Ile variant. This variant also segregated in all additional family members previously not included in the linkage study. At the same position another amino acid change p.Thr132Ser was listed in dbSNP database (rs143473232), this variant is present in 1 of 13 006 chromosomes in the EVS.

In Family B, linkage analysis revealed five plausible regions with suggestive but inconclusive linkage (LOD score >1) on chromosomes 5, 6, 11, 13 and 14.

Searching these five regions of interest for variants identified by whole-exome sequencing in the index patients, promising variants in six candidate genes were found: *CDC42BPG*, *KLHDC1*, *MYH7*, *PYGL*, *PCDHB1*, and the p.Pro134His variation in *HARS* as the most likely segregating candidate.

In Family C, whole-exome sequencing data filtering yielded promising variants in 66 genes including a p.Asp175Glu variant in *HARS*, which was found to segregate with the disease in the pedigree.

In Family D, linkage analysis including seven affected and five healthy individuals delineated six genomic regions of interest: four on chromosomes 4, 5, 8, 9 (LOD score 2.4) and two located on the X chromosome (LOD score 1.8). Whole-exome sequencing data from two affected patients combined with linkage analysis revealed only two possible variants, one in *LHX6* and one in *HARS*. After confirmation with Sanger sequencing, the variant in *LHX6* was excluded because of presence also in a healthy family member not included in the original linkage analysis, thus leaving the segregating p.Asp364Tyr variant in *HARS* as the only probable disease cause.

All variants detected in *HARS* (p.Thr132Ile, p.Pro134His, p.Asp175Glu, p.Asp364Tyr) are in the heterozygous state and segregate with disease in all available family members from Families A–D (Fig. 1). *In silico* prediction programs classified all four missense variants as pathogenic: 'probably damaging' (PolyPhen-2) (Adzhubei *et al.*, 2010), 'damaging' (SIFT) (Ng and Henikoff, 2001), 'disease causing' (Mutation Taster) (Schwarz *et al.*, 2014) and 'high' (Mutation Assessor) (Reva *et al.*, 2011). The same apply also for the variant p.Thr132Ser; the prediction programs assessed it as pathogenic. None of the four *HARS* variants are present in dbSNP, the Exome Variant Server, or 1000 genomes database (Supplementary Table 2). No additional *HARS* mutations were found in a cohort of 62 index patients with genetically unresolved HMN to which Family D belonged. Families B, C, and D were part of large whole-exome sequencing effort tackling a heterogeneous cohort of 128 autosomal dominant families with genetically undefined neuropathies (axonal and intermediate CMT and

HMN). Data were analysed using GEMapp (Gonzalez *et al.*, 2013b) but apart from these three families, no additional *HARS* mutations were identified.

Clinical findings

Clinical and electrophysiological findings in all studied individuals are summarized in Table 1 and Supplementary Table 3. Photos of selected patients from Families A and D are in Supplementary Fig. 1. The phenotype is variable, with disease onset ranging from early childhood to late adulthood. Some individuals had clinical signs and electrophysiological abnormalities without subjective symptoms (Subjects A-IV.3, A-IV.6, D-IV.2, and D-IV.6). Especially in Family D, most patients are mildly affected, often only displaying steppage gait and sensory symptoms/signs at later stages of the disease (Supplementary Fig. 1). Two asymptomatic individuals (Subjects D-IV.2 and D-IV.6) have brisk patellar reflexes with absent ankle jerks. Based on electrophysiological studies, the phenotypes of the families were classified as axonal neuropathy in Families A, C, and D and intermediate neuropathy in Family B. Four young individuals did not have sensory symptoms/signs and normal sensory nerve conduction studies consistent with a diagnosis of HMN (Subjects A-V.1, D-IV.2, D-IV.3 and D-IV.6). Older individuals of the same families were diagnosed with CMT2.

HTS1 mutations are associated with decreased cell viability in yeast

Yeast complementation assays have been employed to test mutations in *ARS* genes for a loss-of-function effect, including p.Arg137Gln in *HARS* (Antonellis *et al.*, 2006; Jordanova *et al.*, 2006; McLaughlin *et al.*, 2010; Stum *et al.*, 2011; Gonzalez *et al.*, 2013a; Vester *et al.*, 2013; Griffin *et al.*, 2014). To test the functional consequences of the four *HARS* missense variants that segregate with disease (p.Thr132Ile, p.Pro134His, p.Asp175Glu and p.Asp364Tyr) and one rare variant listed in dbSNP without diseases association (p.Thr132Ser), we modelled these missense variants in the yeast orthologue *HTS1* (Supplementary Table 4) and independently tested each mutation for the ability to support yeast cell growth compared to wild-type *HTS1* or an empty vector. Mutations in the text and Fig. 2 are referred to by the position in the human protein. Briefly, a haploid yeast strain (with the endogenous *HTS1* locus deleted and a maintenance vector to express wild-type *HTS1* and *URA3*) was transformed with either a pRS315 vector with no insert ('Empty pRS315' in Fig. 2) or a pRS315 vector harbouring wild-type, p.Thr132Ile, p.Thr132Ser, p.Pro134His, p.Asp175Glu, or p.Asp364Tyr *HTS1*. Yeast cells were then selected on media containing 5-FOA, which is toxic to yeast expressing *URA3* and therefore selects for cells that have spontaneously lost the maintenance vector (Boeke *et al.*, 1987). Only yeast cells expressing a

functional *HTS1* allele from pRS315 will grow in this assay.

Yeast transformed with a wild-type *HTS1* expression vector demonstrated significant growth, while those transformed with the empty vector did not (Fig. 2). These data are consistent with *HTS1* being an essential gene (Vester *et al.*, 2013). Regarding the novel, CMT-associated *HARS* mutations described here, yeast expressing p.Thr132Ile, p.Pro134His and p.Asp364Tyr *HTS1* were unable to grow on 5-FOA media (Fig. 2) indicating that these are complete loss-of-function alleles. Additionally, yeast expressing p.Asp175Glu *HTS1* showed a significant reduction, but not complete abrogation, of yeast viability compared to wild-type *HTS1* (Fig. 2; note pronounced differences in growth at 1:10 and 1:100 dilutions) indicating that this is a partial loss-of-function allele. Unlike CMT-associated *HARS* mutations, the p.Thr132Ser *HARS* variant supported yeast growth to the same extent as wild-type *HARS*, indicating that this variant has no significant effect on *HARS* activity.

p.Asp364Tyr causes late-onset motor neuron defects and behavioural impairments in *C. elegans*

C. elegans was previously established as a model system to differentiate the pathogenicity of potential mutant *hars-1* (the *C. elegans* orthologue of *HARS*) variants (Vester *et al.*, 2013). In *C. elegans*, 19 GABA motor neurons innervate body wall muscles and are required for locomotion via reciprocal inhibition (Schuske *et al.*, 2004). These GABA motor neuron cell bodies reside in the ventral nerve cord and extend circumferential axons that form the dorsal nerve cord—these axons are easily visualized with fluorescent proteins facilitating visual assessment of axon morphology and integrity (Fig. 3A). To determine if p.Asp364Tyr expression resulted in morphological and functional toxicity to motor neurons, we specifically expressed the *C. elegans hars-1* (p.Asp364Tyr) transgene in GABA motor neurons, which were labelled with green fluorescent protein (GFP). Expression of p.Asp364Tyr caused morphological neurotoxicity denoted by dorsal and ventral nerve gaps, axonal blebbing, and severely aberrant axonal processes that were not present in control animals (Fig. 3B). Axonal morphological defects increased over time (L4 to 7-day adult) in those animals expressing the p.Asp364Tyr variant (Fig. 3C). To determine if the axonal pathology produced behavioural defects, we tested animals in liquid thrash assays, which measure the fidelity of neuromuscular motor performance (Miller *et al.*, 1996). Transgenic animals expressing the p.Asp364Tyr variant exhibited significantly decreased thrashing rates compared to control in 4- and 7-day adults, which mirrored the increased axonal pathology (Fig. 3D). Although p.Asp364Tyr expressing L4 and 1-day adult animals exhibited a significant increase in axonal pathology, there were no overt behavioural defects,

Table 1 Clinical findings in patients with HARS mutations

Individual (mutation, origin)	Onset (age, years)	Disease duration, years	Walking	Weakness (proximal/distal)	Sensory loss	Other features	NCS
A-III.3 p.Thr132Ile German	Weakness of foot dorsiflexion (25)	15	Steppage gait, no aids	UL 5/5 LL 5/2	Reduced vibration sense distally (LL)	Pes cavus	CMT2
A-III.5	Pes cavus, hammer toes (childhood)	60	Steppage, uses wheeled walker	UL 5/3 LL 4/0	Distal loss of vibration sense (LL)	Pes cavus	CMT2
A-IV.3	No complaints at age 62	No	Mild steppage gait, no aids	UL 5/5- LL 5/3	Reduced vibration sense distally (LL)	Pes cavus	CMT2
A-IV.4	Slender hands and feet (childhood)	40	Steppage, no aids	UL 5/4 LL 5/2	Hypoesthesia of the feet, vibration sense reduced distally (LL)	Pes cavus	CMT2
A-IV.6	No complaints at age 58	No	Normal gait, no heel walking	UL 5/5 LL 5/4	Distal loss of vibration sense (LL)	Pes cavus	CMT2
A-IV.7	Weakness in his hands (26)	10	Normal gait, is still able to walk on heels a few steps	UL 5/3 LL 5/4	Hypoesthesia of the 1st toe, reduced vibration sense distally (LL)	Pes cavus	CMT2
A-V.1	Weakness in his hands, hammer toes (20)	4	Normal gait, no heel walking	UL 5/4 LL 5/4	No	No	HMN
B-II.2 p.Pro134His Moroccan	Gait difficulties (childhood)	> 40	Severe steppage, crutch	UL 5/3 LL 5/0	Panmodal distal	No	CMT1
B-II.5	Gait difficulties (childhood)	> 35	Steppage, no aids	UL 5/4 LL 4+/2	Distal loss of vibration and pinprick sense	Hip dysplasia R	CMT1
B-III.3	Gait difficulties (10)	7	Steppage, no aids	UL 5/4+ LL 5/1	Distal loss of vibration sense (LL)	No	CMT2/CMT-INT
B-III.5	Gait difficulties, weakness hands (> 20)	> 8	Slight steppage, no aids	UL 5/4+ LL 5-/4-	Distal paresthesia and loss of vibration sense (LL)	No	CMT-INT
C-I.1 p.Asp175Glu Czech/Belgian	Subjectively no weakness at age 80	No	No heel walking	UL 4/3+ LL 4/3+	Reduced distal vibration sense (LL), cold feet	Brisk patellar reflexes	CMT2
C-II.1	Pain, positive sensor symptoms (39)	8	Is able walk on heels and tiptoes	UL 5/5 LL 5/4	Reduced distal vibration sense (LL), cold feet	No	CMT2
C-II.2	Pain, positive sensor symptoms (> 37)	11	Slight steppage, no aids	UL 5/5- LL 5/4	Distal dysaesthesia and reduced vibration sense (LL)	Intact/brisk reflexes	CMT2
C-III.1	Foot deformities (12)	15	Steppage, in-soles, no other aids	UL 5/5- LL 5/2	Distal, panmodal	Pes cavus/hammer toes	CMT2
D-II.2 p.Asp364Tyr Czech	Gait difficulties (20)	56	Steppage, crutches	UL 5/3+ LL 5/0	Distal panmodal	Areflexia, atrophic intrinsic hand muscles	(CMT)
D-III.2	Gait difficulties (26)	21	Steppage	UL 5/5 LL 5/0	Distal reduced vibration sense and hypaesthesia	Brisk patellar reflexes	CMT2
D-III.4	Gait difficulties (19)	34	Steppage, crutches	UL 5/4 LL 5/0	Hypaesthesia distal, Reduced vibration sense	Areflexia (LL)	(CMT)

(continued)

Table 1 Continued

Individual (mutation, origin)	Onset (age, years)	Disease duration, years	Walking	Weakness (proximal/distal)	Sensory loss	Other features	NCS
D-IV.1	Gait difficulties (15)	14	Steppage	UL 5/5 LL 5/3	Reduced distal vibration sense	Brisk patellar reflexes, absent ankle jerks, atrophic intrinsic hand muscles	CMT2
D-IV.2	Asymptomatic (21)	No	Normal	UL 5/5 LL 5/5	No	Brisk patellar reflexes, absent ankle jerks	HMN
D-IV.3	Gait difficulties (20)	8	Steppage	UL 5/5 LL 5/1	No	Brisk patellar reflexes, absent ankle jerks	HMN
D-IV.6	Asymptomatic (32)	No	Normal	UL 5/5 LL 5/5	No	Brisk patellar reflexes, absent ankle jerks	HMN

UL = upper limb; LL = lower limb; NCS = nerve conduction study; muscle strength according to MRC scale, the lowest score is shown for the proximal and distal aspect of the limb, separated by /; CMT1/CMT2/CMT INT/HMN, Charcot-Marie-Tooth disease type 1, type 2 and intermediate type, hereditary motor neuropathy (type between brackets if based on clinical finding but NCS not available).

suggesting p.Asp364Tyr expression imparts a progressive loss of motor neuron function and neuromuscular coordination (Fig. 3C and D).

Discussion

The advent of next-generation, high-throughput sequencing technologies has allowed rapid identification of disease-associated variants. However, these same advances have caused human geneticists to be increasingly faced with variants of unknown significance in single patients and small families (Schabhuettl *et al.*, 2014). Several ARS family members have been implicated in IPNs; however, the simple identification of a missense variant in a gene encoding one of these enzymes is not sufficient evidence of pathogenicity. To date, mutations in three ARSs (*GARS*, *YARS* and *AARS*) have strong genetic evidence supporting a role in dominantly inherited peripheral neuropathy (Antonellis *et al.*, 2003; Jordanova *et al.*, 2006; Latour *et al.*, 2010; Zhao *et al.*, 2012). Our study now establishes the same level of genetic evidence for the role of *HARS* in IPN. Previously, a missense variant in histidyl-tRNA synthetase (p.Arg137Gln *HARS*) was identified in a single patient with late-onset, sensory-predominant axonal neuropathy; however, segregation studies could not be performed and this variant was also identified at a very low rate in the general population (Vester *et al.*, 2013). Despite demonstrating a loss of function and dominant toxicity in established functional assays, the lack of segregation studies and failure to identify additional unrelated families with IPN and *HARS* mutations made it difficult to establish a causal link between *HARS* and IPN (Vester *et al.*, 2013). In the current study, next-generation sequencing was used to identify four *HARS* mutations in four large unrelated families with IPN. All four mutations are missense alterations that segregate with disease status and that are predicted to be pathogenic using several *in silico* tools (Supplementary Table 2). In the current study no large systematic cohort screenings have been performed so an accurate estimation of *HARS* mutation frequencies is not possible. Based on the series that were studied we estimate that the frequency is in the order of 1.6–2.3% (1/62 in HMN cases and 3/128 in GEMapp). Given the extensive phenotypic diversity associated with *HARS* mutations we expect multiple additional cases are likely to be identified in future whole-exome sequencing studies.

A growing body of evidence suggests that impaired enzyme function is an important component of ARS-mediated CMT disease. Fifteen of 19 CMT-associated mutations in *GARS*, *YARS*, and *AARS* demonstrate loss-of-function characteristics in aminoacylation assays and/or in yeast complementation assays. Importantly, all mutations that cause a loss of function in yeast growth assays also demonstrate loss of tRNA charging in kinetic assays (Jordanova *et al.*, 2006; McLaughlin *et al.*, 2010, 2012; Griffin *et al.*, 2014). By using a yeast model to test the

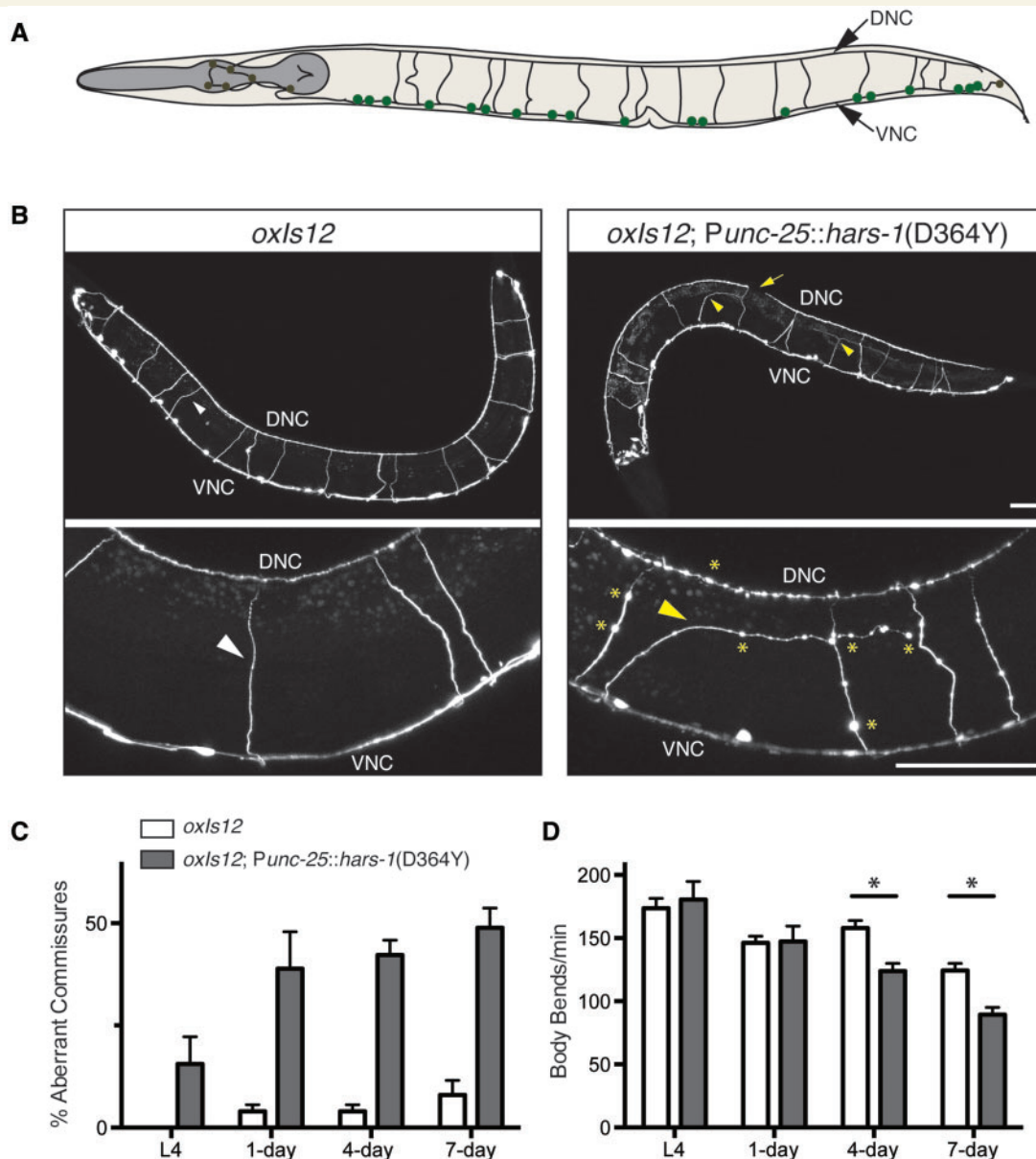


Figure 3 p.Asp364Tyr (D364Y) motor neuron expression causes axonal pathology and neuromuscular defects in *C. elegans*. (A) Diagram of the 19 DD and VD GABA motor neuron cell bodies (green dots), which are located in the ventral nerve cord (VNC), and their commissural axonal processes. Ventral motor neuron cell bodies extend dorsal circumferential axons forming the dorsal nerve cord (DNC). Figure adapted with permission from Vester *et al.* (2013). (B) Whole animal (*upper panels*) and magnified (*lower panels*) confocal images of control *oxls12* [*Punc-47::GFP*] and *oxls12; hars-1* (D364Y) expressing animals. In control animals, commissural axons (white arrowhead) extend dorsally from ventral motor neuron cell bodies forming a continuous dorsal nerve cord. Note the homogeneous GFP expression and lack of axonal blebbing in control animals (*lower panel*, white arrowhead). Expression of *hars-1* (D364Y) causes aberrant axonal commissures that fail to reach the dorsal nerve cord (yellow arrowhead), prominent dorsal nerve cord gaps (yellow arrow), and axonal blebbing (yellow asterisks) not observed in controls. Scale bar = 50 μ m. (C) Quantification of aberrant GABA motor neuron axonal commissures in HARS-I (D364Y) expressing animals ($n \geq 100$ worms/genotype; $n = 5$ trials/genotype). (D) Quantification of thrash assays in liquid media ($n \geq 40$ animals/genotype). Error bars \pm SEM, * $P < 0.05$, Students *t*-test.

function of ARS variants *in vivo*, we determined that all four disease-associated HARS variants result in a severe reduction in yeast viability. In contrast, although affecting the same residue as p.Thr132Ile, the p.Thr132Ser HARS variant, which is not associated with disease, complements loss of endogenous HTS1, indicating that p.Thr132Ser is

not a loss-of-function allele (Fig. 2). This supports the notion that impaired function is an important component of ARS-mediated disease pathogenesis. In addition, we used a *C. elegans* model to show that over-expression of p.Asp364Tyr HARS causes morphological and functional motor deficits, consistent with the dominant IPN phenotype

observed in patients carrying this mutation. This also confirms that yeast and *C. elegans* data are consistent with the previously identified variant (Vester *et al.*, 2013) and in favour of pathogenicity allowing the use of genetic and yeast data alone to implicate the remaining alleles.

Phenotypic diversity in IPN is well documented and next generation sequencing techniques have helped reveal the allelic heterogeneity of IPN-associated mutations that may, at least partially, explain the phenotypic variations observed. Our current study demonstrates the diverse types of IPN—in terms of presentation, severity and electrophysiology—that are associated with *HARS* mutations. Family A is diagnosed with an adult onset CMT2 phenotype of moderate severity. Family B on the other hand displays a more severe disease course with marked slowing of nerve conduction velocities that are in the range of CMT1 for the older individuals. This finding suggests a progressive slowing of nerve conduction velocities. Subject B-III.5 had positive sensory symptoms under the form of paraesthesia. In Family C the disease presentation and severity is highly variable with the male index (Subject C-III.1) presenting a typical CMT phenotype in adolescence while his mother (Subject C-II.2) has unusual late onset features with positive sensory symptoms. Electrophysiology is again in keeping with CMT2 although the effect of progressive slowing of nerve conduction velocities seems to be present as well. In Family D, an initial diagnosis of pure motor axonal neuropathy was made in some patients (HMN) but on progression of the disease in older individuals, clear sensory symptoms and signs and abnormalities of the sensory nerve conduction were noted. Follow-up over time will show if sensory involvement becomes apparent in Subjects A-V.1, D-IV.2, D-IV.3 and D-IV.6 as well. Most other neuropathy phenotypes associated with mutations in the ARSs genes have an axonal electrophysiology with the exception of DI-CMTC caused by *YARS* mutations where a degree of nerve conduction velocity slowing in the intermediate range is described (Jordanova *et al.*, 2006). Even within the group of axonal neuropathies linked to the ARS genes clear, variability of the affected nerve fibres is known with *GARS* and *AARS* mutations causing both CMT2 and HMN phenotypes (Antonellis *et al.*, 2003; Zhao *et al.*, 2012). For the currently described *HARS* mutations, no obvious genotype–phenotype correlations can be made. The Asp175Gly mutation in *HARS* is a hypomorphic allele with a clearly reduced but not completely abolished yeast colony growth compared to control conditions. Given the mildly affected individuals in the first and second generation of the corresponding family this raises the question of a genotype–phenotype correlation. However Subject C-III.1 has a more typical CMT phenotype in adolescence so this correlation is certainly not straightforward. At the same time several individuals in Family A (Subjects A-IV.3 and A-IV.6) and Family D (Subjects D-IV.2 and D-IV.6) are very mildly affected as well although their respective mutations (Thr132Ile and Asp364Tyr) are complete loss of function alleles. Based on this observation and also our

extensive previous experience with other ARS genes (*GARS* and *AARS*), we are confident that the yeast assay is a robust predictor of disease but does not allow for strong correlations with disease severity.

ARSs are ubiquitously expressed enzymes that perform the essential first step of protein translation. It is therefore interesting that mutations in genes encoding these enzymes have been implicated in tissue-specific diseases such as peripheral neuropathy. There is currently a preponderance of data suggesting that impaired ARS function is a component of dominant ARS-related IPN; however, to date only missense and in-frame deletions have been associated with these diseases suggesting that the mutant protein must be expressed. This apparent discrepancy may be explained by two non-mutually exclusive possibilities. First, as *GARS*, *AARS*, *YARS*, and *HARS* holoenzymes function as homodimers, the loss-of-function protein may deplete the function of the remaining wild-type protein via a dominant-negative effect (Freist *et al.*, 1999). In this scenario, dramatically reduced ARS function may breach a threshold of tRNA charging required for protein translation in axons, leading to the axonal phenotype (Wallen and Antonellis, 2013). Second, impaired ARS function (i.e. reduced catalytic activity or decreased tRNA binding) may be a prerequisite for an as-yet undiscovered toxic gain-of-function effect; for example, mutant ARS may now be free to inappropriately bind to axonal RNAs or proteins (Motley *et al.*, 2010, 2011; Wallen and Antonellis, 2013). The first possibility is supported by the over 20 loss-of-function mutations identified in the dimeric *GARS*, *YARS*, *AARS* and *HARS* enzymes in patients with IPN (Wallen and Antonellis, 2013; Griffin *et al.*, 2014) and the fact that each *HARS* mutation described here maps to the catalytic domain of the enzyme. The second possibility is supported by the apparent lack of a neuropathy phenotype in patients with Usher Syndrome that are homozygous for a presumably hypomorphic *HARS* mutation (p.Tyr454Ser) (Puffenberger *et al.*, 2012). However, it is important to note that patients homozygous or compound heterozygous for null and/or hypomorphic mutations in other ARS enzymes do present with a peripheral neuropathy (Isohanni *et al.*, 2010; McLaughlin *et al.*, 2010; Schwartztruber *et al.*, 2014). While the mechanistic link between ARS mutations and IPN remains unclear, there is abundant evidence that reduced ARS function is an important component of the molecular pathology.

Here we present clinical, genetic and functional data that implicate *HARS* mutations in inherited peripheral neuropathy. These findings expand the locus, allelic, and phenotypic spectrum of ARS-related human disease and further support a pathogenic role for these enzymes in diseases of the peripheral nerve. Future efforts aimed at teasing out the precise molecular pathology of ARS mutations will be critical for assessing if improving enzyme function or decreasing the activity of mutant ARS alleles will be relevant therapeutic strategies for patients with dominant ARS-related disease.

Acknowledgements

We would like to thank all the patients and participants of the study for their cooperation.

Funding

This study was supported by IGA MH CZ No. NT 14348-3 and MH CZ - DRO, University hospital Motol, Prague, Czech Republic 00064203, a grant from the Muscular Dystrophy Association (MDA294479) to A.A. and A.A.B. Further support was provided by the National Institutes of Health Cellular and Molecular Biology Training Grant (T32 GM007315), the National Institutes of Health Medical Scientist Training Grant (T32 GM007863) and National Institutes of Health Grant F30 NS092238 to L.B.G. Further support came from the University of Antwerp (UA), the Association Belge contre les Maladies Neuromusculaires (ABMM) and the EU FP7/2007-2013 under grant agreement number 2012-305121 (NEUROMICS). This work was supported by NIH (R01NS075764 and U54NS065712 SZ) and the CMT Association. Additional support was provided by the Swiss National Science Foundation (Grant Number 310030_156260) and the Gebert-Rüf Foundation (Rare Diseases – New Technologies Grant) to C.R.

Supplementary material

Supplementary material is available at *Brain* online.

References

- Abecasis GR, Cherny SS, Cookson WO, Cardon LR. Merlin-rapid analysis of dense genetic maps using sparse gene flow trees. *Nat Genet* 2002; 30: 97–101.
- Adzhubei IA, Schmidt S, Peshkin L, Ramensky VE, Gerasimova A, Bork P, et al. A method and server for predicting damaging missense mutations. *Nat Methods* 2010; 7: 248–9.
- Antonellis A, Ellsworth RE, Sambughin N, Puls I, Abel A, Lee-Lin SQ, et al. Glycyl tRNA synthetase mutations in Charcot-Marie-Tooth disease type 2D and distal spinal muscular atrophy type V. *Am J Hum Genet* 2003; 72: 1293–9.
- Antonellis A, Green ED. The role of aminoacyl-tRNA synthetases in genetic diseases. *Ann Rev Genomics Hum Genet* 2008; 9: 87–107.
- Antonellis A, Lee-Lin SQ, Wasterlain A, Leo P, Quezado M, Goldfarb LG, et al. Functional analyses of glycyl-tRNA synthetase mutations suggest a key role for tRNA-charging enzymes in peripheral axons. *J Neurosci* 2006; 26: 10397–406.
- Baets J, De Jonghe P, Timmerman V. Recent advances in Charcot-Marie-Tooth disease. *Curr Opin Neurol* 2014; 27: 532–40.
- Boeke JD, Trueheart J, Natsoulis G, Fink GR. 5-Fluoroorotic acid as a selective agent in yeast molecular genetics. *Methods Enzymol* 1987; 154: 164–75.
- Brenner S. The genetics of *Caenorhabditis elegans*. *Genetics* 1974; 77: 71–94.
- Freist W, Verhey JF, Ruhlmann A, Gauss DH, Arnez JG. Histidyl-tRNA synthetase. *Biol Chem* 1999; 380: 623–46.
- Gonzalez M, McLaughlin H, Houlden H, Guo M, Yo-Tsen L, Hadjivassiliou M, et al. Exome sequencing identifies a significant variant in methionyl-tRNA synthetase (MARS) in a family with late-onset CMT2. *J Neurol Neurosurg Psychiatry* 2013a; 84: 1247–9.
- Gonzalez MA, Lebrigio RF, Van Booven D, Ulloa RH, Powell E, Speziani F, et al. GENomes Management Application (GEM.app): a new software tool for large-scale collaborative genome analysis. *Hum Mutat* 2013b; 34: 842–6.
- Griffin LB, Sakaguchi R, McGuigan D, Gonzalez MA, Searby C, Zuchner S, et al. Impaired function is a common feature of neuropathy-associated Glycyl-tRNA Synthetase mutations. *Hum Mutat* 2014; 35: 1369–71.
- Harding AE, Thomas PK. The clinical features of hereditary motor and sensory neuropathy types I and II. *Brain* 1980; 103: 259–80.
- Isohanni P, Linnankivi T, Buzkova J, Lonqvist T, Pihko H, Valanne L, et al. DARS2 mutations in mitochondrial leucoencephalopathy and multiple sclerosis. *J Med Genet* 2010; 47: 66–70.
- Jordanova A, Irobi J, Thomas FP, Van Dijk P, Meerschaert K, Dewil M, et al. Disrupted function and axonal distribution of mutant tyrosyl-tRNA synthetase in dominant intermediate Charcot-Marie-Tooth neuropathy. *Nat Genet* 2006; 38: 197–202.
- Latour P, Thauvin-Robinet C, Baudalet-Mery C, Soichot P, Cusin V, Faivre L, et al. A major determinant for binding and aminoacylation of tRNA(Ala) in cytoplasmic Alanyl-tRNA synthetase is mutated in dominant axonal Charcot-Marie-Tooth disease. *Am J Hum Genet* 2010; 86: 77–82.
- McLaughlin HM, Sakaguchi R, Giblin W, Wilson TE, Biesecker L, Lupski JR, et al. A recurrent loss-of-function alanyl-tRNA synthetase (AARS) mutation in patients with Charcot-Marie-Tooth disease type 2N (CMT2N). *Hum Mutat* 2012; 33: 244–53.
- McLaughlin HM, Sakaguchi R, Liu C, Igarashi T, Pehlivan D, Chu K, et al. Compound heterozygosity for loss-of-function lysyl-tRNA synthetase mutations in a patient with peripheral neuropathy. *Am J Hum Genet* 2010; 87: 560–6.
- Mello CC, Kramer JM, Stinchcomb D, Ambros V. Efficient gene transfer in *C.elegans*: extrachromosomal maintenance and integration of transforming sequences. *EMBO J* 1991; 10: 3959–70.
- Miller KG, Alfonso A, Nguyen M, Crowell JA, Johnson CD, Rand JB. A genetic selection for *Caenorhabditis elegans* synaptic transmission mutants. *Proc Natl Acad Sci USA* 1996; 93: 12593–8.
- Motley WW, Seburn KL, Nawaz MH, Miers KE, Cheng J, Antonellis A, et al. Charcot-Marie-Tooth-linked mutant GARS is toxic to peripheral neurons independent of wild-type GARS levels. *PLoS Genet* 2011; 7: e1002399.
- Motley WW, Talbot K, Fischbeck KH. GARS axonopathy: not every neuron's cup of tRNA. *Trends Neurosci* 2010; 33: 59–66.
- Murphy SM, Laura M, Fawcett K, Pandraud A, Liu YT, Davidson GL, et al. Charcot-Marie-Tooth disease: frequency of genetic subtypes and guidelines for genetic testing. *J Neurol Neurosurg Psychiatry* 2012; 83: 706–10.
- Ng PC, Henikoff S. Predicting deleterious amino acid substitutions. *Genome Res* 2001; 11: 863–74.
- Puffenberger EG, Jinks RN, Sougnez C, Cibulskis K, Willert RA, Achilly NP, et al. Genetic mapping and exome sequencing identify variants associated with five novel diseases. *PLoS One* 2012; 7: e28936.
- Reva B, Antipin Y, Sander C. Predicting the functional impact of protein mutations: application to cancer genomics. *Nucleic Acids Res* 2011; 39: e118.
- Rosser AM, Polke JM, Houlden H, Reilly MM. Clinical implications of genetic advances in Charcot-Marie-Tooth disease. *Nat Rev Neurol* 2013; 9: 562–71.
- Rozen S, Skaletsky H. Primer3 on the WWW for general users and for biologist programmers. *Methods Mol Biol* 2000; 132: 365–86.
- Saporta AS, Sottile SL, Miller LJ, Feely SM, Siskind CE, Shy ME. Charcot-Marie-Tooth disease subtypes and genetic testing strategies. *Ann Neurol* 2011; 69: 22–33.

- Schabhuttl M, Wieland T, Senderek J, Baets J, Timmerman V, De Jonghe P, et al. Whole-exome sequencing in patients with inherited neuropathies: outcome and challenges. *J Neurol* 2014; 261: 970–82.
- Schuske K, Beg AA, Jorgensen EM. The GABA nervous system in *C. elegans*. *Trends Neurosci* 2004; 27: 407–14.
- Schwartzentruber J, Buhas D, Majewski J, Sasarman F, Papillon-Cavanagh S, Thiffaut I, et al. Mutation in the nuclear-encoded mitochondrial isoleucyl-tRNA synthetase IARS2 in patients with cataracts, growth hormone deficiency with short stature, partial sensorineural deafness, and peripheral neuropathy or with Leigh syndrome. *Hum Mutat* 2014; 35: 1285–9.
- Schwarz JM, Cooper DN, Schuelke M, Seelow D. MutationTaster2: mutation prediction for the deep-sequencing age. *Nat Methods* 2014; 11: 361–2.
- Skre H. Genetic and clinical aspects of Charcot-Marie-Tooth's disease. *Clin Genet* 1974; 6: 98–118.
- Stum M, McLaughlin HM, Kleinbrink EL, Miers KE, Ackerman SL, Seburn KL, et al. An assessment of mechanisms underlying peripheral axonal degeneration caused by aminoacyl-tRNA synthetase mutations. *Mol Cell Neurosci* 2011; 46: 432–43.
- Vester A, Velez-Ruiz G, McLaughlin HM, Lupski JR, Talbot K, Vance JM, et al. A loss-of-function variant in the human histidyl-tRNA synthetase (HARS) gene is neurotoxic *in vivo*. *Hum Mutat* 2013; 34: 191–9.
- Wallen RC, Antonellis A. To charge or not to charge: mechanistic insights into neuropathy-associated tRNA synthetase mutations. *Curr Opin Genet Dev* 2013; 23: 302–9.
- Zhao Z, Hashiguchi A, Hu J, Sakiyama Y, Okamoto Y, Tokunaga S, et al. Alanyl-tRNA synthetase mutation in a family with dominant distal hereditary motor neuropathy. *Neurology* 2012; 78: 1644–9.